

# Modeling and Simulation of Oxygen-Limited Partial Nitrification in a Membrane-Assisted Bioreactor (MBR)

Stijn Wyffels,<sup>1</sup> Stijn W. H. Van Hulle,<sup>2</sup> Pascal Boeckx,<sup>1</sup> Eveline I. P. Volcke,<sup>2</sup> Oswald Van Cleemput,<sup>1</sup> Peter A. Vanrolleghem,<sup>2</sup> Willy Verstraete<sup>3</sup>

<sup>1</sup>Laboratory for Applied Physical Chemistry, Faculty of Agricultural and Applied Biological Sciences, Ghent University, Coupure Links 653, B-9000 Gent, Belgium; telephone: + 32 (9) 264 60 00; fax: + 32 (9) 264 62 30; e-mail: [stijn.wyffels@ugent.be](mailto:stijn.wyffels@ugent.be)

<sup>2</sup>Department of Applied Mathematics, Biometrics and Process Control (BIOMATH), Faculty of Agricultural and Applied Biological Sciences, Ghent University, Coupure Links 653, B-9000 Gent, Belgium

<sup>3</sup>Laboratory for Microbial Ecology and Technology (LabMET), Faculty of Agricultural and Applied Biological Sciences, Ghent University, Coupure Links 653, B-9000 Gent, Belgium

Received 2 September 2003; accepted 22 December 2003

Published online 8 April 2004 in Wiley InterScience ([www.interscience.wiley.com](http://www.interscience.wiley.com)). DOI: 10.1002/bit.20008

**Abstract:** Combination of a partial nitrification process and an anaerobic ammonium oxidation process for the treatment of sludge reject water has some general cost-efficient advantages compared to nitrification–denitrification. The integrated process features two-stage autotrophic conversion of ammonium via nitrite to dinitrogen gas with lower demand for oxygen and no external carbon requirement. A nitrifying membrane-assisted bioreactor (MBR) for the treatment of sludge reject water was operated under continuous aeration at low dissolved oxygen (DO) concentrations with the purpose of generating nitrite accumulation. Microfiltration was applied to allow a high sludge retention time (SRT), resulting in a stable partial nitrification process. During start-up of the MBR, oxygen-limited conditions were induced by increasing the ammonium loading rate and decreasing the oxygen transfer. At a loading rate of  $0.9 \text{ kg N m}^{-3} \text{ d}^{-1}$  and an oxygen concentration below  $0.1 \text{ mg DO L}^{-1}$ , conversion to nitrite was close to 50% of the incoming ammonium, thereby yielding an optimal effluent within the stoichiometric requirements for subsequent anaerobic ammonium oxidation. A mathematical model for ammonium oxidation to nitrite and nitrite oxidation to nitrate was developed to describe the oxygen-limited partial nitrification process within the MBR. The model was calibrated with in situ determinations of kinetic parameters for microbial growth, reflecting the intrinsic characteristics of the ammonium oxidizing growth system at limited oxygen availability and high sludge age. The oxygen transfer coefficient ( $K_L a$ ) and the ammonium-loading rate were shown to be the appropriate operational variables to describe the experimental data accurately. The validated model was used for further steady state simu-

lation under different operational conditions of hydraulic retention time (HRT),  $K_L a$ , temperature and SRT, with the intention to support optimized process design. Simulation results indicated that stable nitrite production from sludge reject water was feasible with this process even at a relatively low temperature of  $20^\circ\text{C}$  with HRT down to 0.25 days. © 2004 Wiley Periodicals, Inc.

**Keywords:** modeling; partial nitrification; MBR; simulation

## INTRODUCTION

Keeping in mind some adverse environmental effects of excess nitrogen and its increasingly stringent discharge standards, specific attention for the abatement of strong nitrogenous wastewater becomes an important issue in today's sustainable treatment plants. For example, in wastewater treatment plants with anaerobic digestion of sewage sludge, dewatering liquor (or reject water) is produced containing 700–1200 mg total ammonium nitrogen (TAN)  $\text{L}^{-1}$  that can account for up to 20% of the plant's total nitrogen loading rate. Side-stream treatment of this reject water by conventional nitrification–denitrification is generally considered as more beneficial than chemical nitrogen elimination by magnesium-ammonium-phosphate precipitation or by air stripping (Siegrist, 1996). However, to achieve complete biological nitrogen removal the denitrification step needs to be supplied with an extra organic carbon source, entailing higher operational costs. As such, new approaches are needed to make nitrogen removal more cost-efficient with less input of resources for a variety of so-called hard-to-treat concentrated streams with unfavorable carbon content. A significantly improved nitrogen removal system is based on the combination of partial nitrification and anaerobic ammonium oxidation. This combined completely

Correspondence to: Stijn Wyffels

Contract grant sponsors: the Flemish region and the Flemish Institute for the Improvement of Scientific-Technological Research in the Industry; European Union

Contract grant numbers: IWT-STWW project 980362; IcoN project no. EVK1-CT2000-054

autotrophic process has great potential since there is no longer need for external carbon addition, sludge production is very low, and oxygen input and aeration energy requirements are largely reduced. The combined autotrophic process can be engineered in an aerobic partial nitrification and an anaerobic ammonium oxidation bioreactor, or implemented in one single system. Separating nitrification and anaerobic ammonium oxidation in two reactors offers the opportunity to control both processes under their optimal conditions that results in lower effluent nitrogen concentrations (Verstraete and Phillips, 1998; Jetten et al., 2002).

The novel anaerobic ammonium oxidation (Anammox) process was discovered nearly 10 years ago and has been extensively investigated and reviewed (Mulder et al., 1995; Jetten et al., 1999). During the anaerobic oxidation of ammonium, nitrite is denitrified to dinitrogen gas in the absence of oxygen with ammonium as the electron donor (van de Graaf et al., 1997). Nitrite can be produced efficiently via nitrification of the ammonium-rich wastewater (Voets et al., 1975).

During nitrification ammonium is oxidized to nitrite only. Partial nitrification refers to the partial (or uncomplete) conversion of ammonium to nitrite. Several practical strategies for nitrite accumulation are described in literature. The SHARON process operates without biomass retention and takes advantage of the relatively high temperature (30–35°C) of fresh sludge reject water. At these temperatures the ammonium oxidizers have higher growth rates than nitrite oxidizers so that by carefully controlling the dilution rate (SRT = HRT, generally around 1 day) the nitrite oxidizers can be selectively washed out resulting in the prevention of nitrite oxidation (Hellinga et al., 1998). The SHARON process was successfully implemented at full scale for the treatment of fresh sludge reject water (Mulder et al., 2001).

Restriction of nitrite oxidizer growth by free ammonia (FA) inhibition can be applied in mixed systems where both groups of nitrifiers are present. Free ammonia concentrations of 1–5 mg NH<sub>3</sub> L<sup>-1</sup> were shown to inhibit nitrite oxidation with only minor effects on ammonium oxidation (Abeling and Seyfried, 1992). Anthonisen et al. (1976) found that the inhibitory concentration of FA is higher for *Nitrosomonas* than for *Nitrobacter* species, with values of 10 and 0.1 mg NH<sub>3</sub> L<sup>-1</sup>, respectively. However, the potential of using only FA inhibition to obtain stable nitrite formation seems somewhat limited since adaptation of the nitrite oxidizing bacteria has been reported (Turk and Mavinic, 1989).

Imposing oxygen limited conditions to outcompete the nitrite oxidizers is generally considered as the most practical alternative in mixed systems with sludge retention. At low oxygen concentration the rate of nitrite oxidation is more adversely affected than the rate of ammonium oxidation, resulting in a sustained accumulation of nitrite. Garrido et al. (1997) reported a biofilm airlift suspension reactor with high loading rates up to 5 kg N m<sup>-3</sup> d<sup>-1</sup>. Under limited oxygen concentrations between 1.5 and 2 mg DO L<sup>-1</sup> full ammonium conversion was maintained with approximately

50% nitrate and 50% nitrite in the reactor effluent. In several other studies nitrite production is linked to oxygen-limited conditions (Bernet et al., 2001; Han et al., 2001; Pollice et al., 2002; Ruiz et al., 2003). In general, the phenomenon of nitrite accumulation is attributed to the often-reported lower oxygen affinity ( $K_O$ ) for nitrite oxidizers than for ammonium oxidizers, making the latter better competitors for limited amounts of oxygen. However, it is also suggested that free hydroxylamine inhibition rather than a difference in affinity constants causes nitrite build-up in nitrifying systems at low oxygen concentration (Yang and Alleman, 1992).

Complete retention of suspended biomass in a membrane-assisted bioreactor (MBR) allowed operation of a high rate nitrification process independently of the sludge growth rate (Wyffels et al., 2003). By adjusting airflow rates and maintaining oxygen-limited conditions, ammonium conversion to nitrite was in the optimal range for further treatment with an Anammox-like process. In this article, the partial nitrification MBR process will be further evaluated through dynamic modeling and simulation. Recently, some studies have been conducted dealing with control and optimization of nitrification processes using two-step nitrification models. Measured nitrification performance and nitrifier community composition in a MBR was compared with simulated data by Liebig et al. (2001). Behavior of the SHARON process was simulated under different operational conditions (Hellinga et al., 1999). To be able to predict the behavior of the MBR in this study, a thoroughly calibrated and validated model would be necessary. With this model optimal operating strategies can be put forward.

The objectives of the present work were therefore threefold: (1) to obtain a steady partial nitrification process which is ideally suited for preceding an anaerobic ammonium oxidation process; (2) to develop a mathematical model which accurately describes the effect of oxygen limitation on ammonium oxidation and nitrite oxidation during start-up of the process; (3) to assess the influence of operating parameters ( $K_L a$ , temperature, HRT, SRT) on the steady-state process performance via simulations with the validated model.

## MATERIALS AND METHODS

### Operation of the MBR for Partial Nitrification

The 1.5-L MBR was operated as a Continuous Stirred Tank Reactor (CSTR) with a submerged microfiltration membrane module (with a total surface of 23 m<sup>2</sup> m<sup>-3</sup> reactor) to allow continuous separation of biomass and reactor effluent (Wyffels et al., 2003). The hollow fiber membranes (Micro PES, Membrana GmbH, Germany) had a maximum pore size of 0.6 μm, thereby retaining all bacterial biomass within the MBR. Apart from sludge removal by sampling no sludge was wasted resulting in a virtual infinite sludge retention time (SRT) of 650 days. After decreasing the HRT during

start-up, a constant HRT of 1 day was maintained by generating a constant membrane flux of  $1.7 \text{ L m}^{-2} \text{ h}^{-1}$ . Reject water from the anaerobic digestion of sewage sludge was used as a source of high strength nitrogen wastewater in these experiments, containing  $931 \pm 122 \text{ mg TAN L}^{-1}$  and  $605 \pm 36 \text{ mg COD L}^{-1}$ . The high bicarbonate content ( $\text{HCO}_3^-/\text{N} = 1.2 \text{ mol mol}^{-1}$ ) of the reject water provided the reactor system with a considerable pH buffering capacity against proton production during ammonium oxidation. To maintain constant operating conditions, the reactor pH was controlled at  $7.90 \pm 0.01$  by adding  $1\text{M NaHCO}_3$ , and the reactor temperature was controlled at  $30.0 \pm 0.1^\circ\text{C}$  by means of a heated water jacket (Biostat B2, Braun Biotech International, Germany). The MBR aeration device consisted of a coarse-bubble air sparging system connected to a flow restrictor for adjusting airflow rates (GasMix, Braun Biotech International, Germany). The mixing system consisted of a double six-blade stirrer, and the stirring rate was controlled at 200 rounds per minute (rpm).

### Chemical Analysis

Concentrations of TAN (Total Ammonium Nitrogen),  $\text{NO}_2\text{-N}$ ,  $\text{NO}_3\text{-N}$  and Chemical Oxygen Demand (COD) were analyzed using spectrophotometric methods (HACH, Cleveland, OH). Mixed liquor suspended solids (MLSS) and volatile suspended solids (VSS) concentration was determined according to standard methods (APHA, 1992). DO (The Dissolved Oxygen) concentration in the MBR was monitored with an Ingold  $\text{pO}_2$  electrode (InPro6100, Mettler-Toledo, Switzerland).

### Batch Determination of Oxygen Transfer Coefficient

The relationship between the airflow rate and the gas–liquid volumetric oxygen transfer coefficient ( $K_La$ ) was determined within the MBR in separate short-term batch experiments, taking 10–33 min depending on the imposed airflow rate. Experiments were conducted at the end of the reactor run under the same operating conditions as for the partial nitrification process, i.e., at a stirring rate of 200 rpm and a temperature of  $30.0^\circ\text{C}$ . After deoxygenation, the medium was re-aerated to oxygen saturation levels and the DO concentration was monitored at different imposed airflow rates, allowing calculation of the  $K_La$  using non-steady state methods (Cornel et al., 2003). Airflow rates were monitored with rotameters and measured with a digital flow meter (ADM1000; J & W Scientific, Folsom, CA).

### Batch Determination of Kinetic and Stoichiometric Parameters for Microbial Growth

Microbial growth parameters were assessed in respirometer batch experiments. Kinetic and stoichiometric parameters of the MBR biomass were determined at  $30.0^\circ\text{C}$  and pH 7.90 at stable operation of the oxygen-limited partial nitrification process after start-up. The MBR was switched to

batch mode, the biomass was washed twice to remove background concentrations and pulses of  $\text{NH}_4\text{Cl}$  and  $\text{KNO}_2$  were added to determine the kinetics the ammonium oxidizing and nitrite oxidizing biomass, respectively. The DO concentration was monitored during the experiments and the calculated oxygen uptake rate (OUR) was used for parameter estimation.

### Model Construction and Simulation

Modeling of the partial nitrification process was performed within the modeling and simulation environment WEST (Vanhooren et al., 2003). The MBR configuration was implemented by placing a CSTR in series with an ideal point-settler with a non-settleable fraction equal to zero, representing the complete retention of biomass. The recycle flow rate of the point-settler to the CSTR was chosen to be very small to prevent possible numerical stiffness of the system (Fig. 1). The  $K_La$  was defined as an operational parameter to describe the effect of varying airflow rates and was controlled through an input file. Other operational and design parameters (temperature, pH, HRT, and influent TAN concentration) were also incorporated in the model via the input file.

Activated Sludge Model #1 (Henze et al., 2000) was chosen as the standard model and was extended with a two-step nitrification model. Bacterial growth and decay processes were modeled for the heterotrophic ( $X_H$ ), and autotrophic ammonium ( $X_{NH}$ ) and nitrite oxidizing ( $X_{NO}$ ) biomass (Table A.II). Endogenous respiration processes were not incorporated within the model because these are not yet clearly documented for ammonium and nitrite oxidizers. Readily degradable substrate ( $S_S$ ) was used for heterotrophic growth. Readily degradable substrate was available from the reject water and was formed through hydrolysis of slowly degradable substrate ( $X_S$ ). The slowly degradable substrate was formed during decay of biomass, along with inert particulate matter ( $X_I$ ) (Table A.I). In the model presented here ammonia ( $S_{NH_3}$ ) rather than ammonium, and nitrous acid ( $S_{HNO_2}$ ) rather than nitrite were used as substrates since these are also the actual substrates for

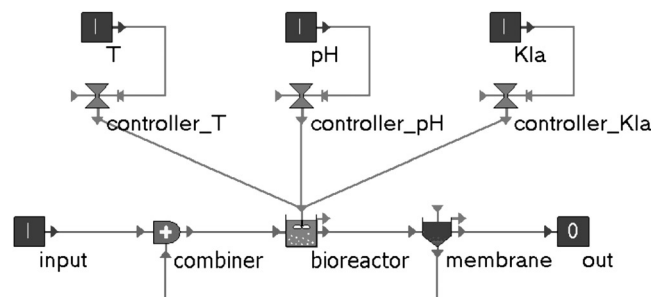


**Figure 1.** Implementation of the MBR configuration in WEST. Operational and design parameters (T, pH, and  $K_La$ ) are defined through an input file (I), as is the influent wastewater composition. The bioreactor is a CSTR with a volume of 1.5 L, while the membrane is mimicked by a point-settler with a non-settleable fraction equal to zero.

ammonium oxidizer and nitrite oxidizer growth, respectively (Anthonisen et al., 1976). The stoichiometry of the reactions was however expressed in terms of corresponding concentrations of TAN ( $S_{NH}$ ) and  $NO_2^-$ -N ( $S_{NO}$ ), as typically done (see calculations in Appendix). Oxygen ( $S_O$ ) was used as electron acceptor for both autotrophic and heterotrophic growth. In addition, denitrifying heterotrophs were using nitrite ( $S_{NO_2}$ ) and nitrate ( $S_{NO_3}$ ) when oxygen became limited. It was assumed that these heterotrophs had no preference for nitrite or nitrate. Therefore similar kinetics were used.

Kinetic and stoichiometric parameters for heterotrophic growth were derived from literature. The substrate affinity constant ( $K_{S,H}$ ) was assumed to be somewhat higher than the reported value of  $20 \text{ mg L}^{-1}$  (Henze et al., 2000), because of the recalcitrant nature of the organic carbon present in the reject water. Similarly, the decay parameters for both heterotrophs and autotrophs were slightly increased to account for the higher decay rates generally observed in nitrifying MBRs (Liebig et al., 2001; Wyffels et al., 2003). An extensive range of parameters for ammonium and nitrite oxidizer growth is reported in literature, mainly determined by the microbial species involved and the operating process conditions. To increase the accuracy of the kinetic model, a combination of experimental data derived specifically for the biomass from the partial nitrification process (operating at low DO and very high SRT) and literature values was used (Table A.III and Table A.IV). A temperature dependency was considered for the  $K_{L,a}$  and for the maximum growth rate ( $\mu^{\max}$ ) and decay rate ( $b$ ). Generally accepted activation energy values, originating from different literature sources were used to calculate the Arrhenius constants for the kinetic parameters (see Appendix).

## RESULTS AND DISCUSSION

### Start-Up and Performance of the Oxygen-Limited Partial Nitrification Process

The MBR was started fresh using a nitrifying inoculum with complete ammonium oxidation to nitrate. Initially, the sludge reject water was supplied at a low ammonium loading rate of  $0.2 \text{ kg N m}^{-3} \text{ d}^{-1}$  for biomass enrichment. The start-up consisted of a stepwise increase of the loading rate (by decreasing the HRT) to a maximum value of  $1.1 \text{ kg N m}^{-3} \text{ d}^{-1}$  and was followed by a gradual decrease of the airflow rate (final  $K_{L,a}$  values between  $130\text{--}160 \text{ d}^{-1}$ ), thereby limiting the oxygen supply to the nitrifying biomass. Increasing the loading rate was performed maintaining complete ammonium oxidation to nitrate, while decreasing the airflow resulted in a concomitant replacement of nitrate by nitrite and accumulation of un-oxidized ammonium. The evolution of HRT and  $K_{L,a}$  during start-up of the partial nitrification process, and the effluent concentration ratios of  $NO_2^-$ -N/ $NO_x^-$ -N and  $NO_2^-$ -N/TAN are shown in Fig. 2a and 2b, respectively. From day 36 onward nitrate is less than

8% of the total oxidized nitrogen species, and after fine-tuning the  $K_{L,a}$  on day 49 the MBR effluent contains nitrite and ammonium at an approximately equimolar ratio. Stable operation of the partial nitrification process treating sludge reject water under oxygen-limited conditions was further maintained for another 3 months (time series not shown). The reactor temperature was kept at  $30.0^\circ\text{C}$ . Strict temperature control at lower values was difficult due to the absence of cooling water in the control system during summer time.

It is suggested that stable accumulation of nitrite when treating high-strength ammonium wastewater with the MBR system is linked to concomitant low DO concentrations and high concentrations of FA (Wyffels et al., 2003). After start-up of the nitrification process by decreasing the HRT and the airflow rate, the DO concentration was below  $0.1 \text{ mg L}^{-1}$ . Nitrite accumulation was also observed under limited oxygen supply in SBR systems independent of SRT, indicating aeration patterns as a possible means to

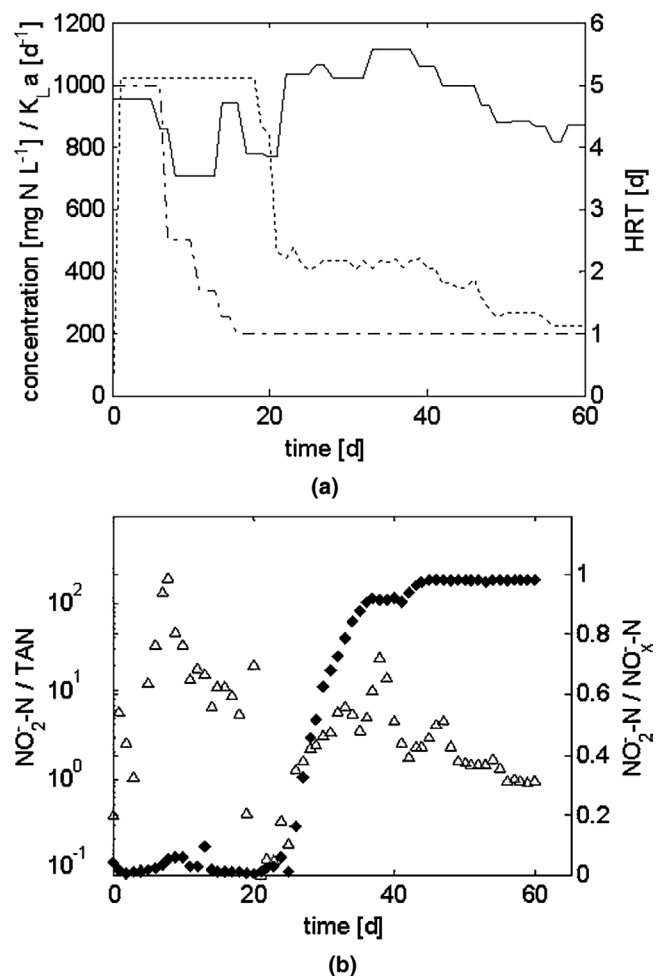


**Figure 2.** (a) Influent ammonium concentration (—), HRT (---) and  $K_{L,a}$  (— · —) profiles during start-up of the partial nitrification process. Gradually decreasing HRT and  $K_{L,a}$  generated oxygen-limited conditions after 21 days. (b) Evolution of the  $NO_2^-$ -N/ $NO_x^-$ -N (◆) and  $NO_2^-$ -N/TAN (△) effluent ratios during start-up of the partial nitrification process.

efficiently control nitrite production from ammonium (Pollice et al., 2002). The pH in the MBR was controlled at pH 7.90, resulting in FA concentrations of 23–26 mg  $\text{NH}_3\text{-N L}^{-1}$ . Therefore, it is most likely that both low DO and high FA contribute to a reduced nitrite oxidizer activity and a consequent stable nitrite production in the partial nitrification MBR.

Nitrite production rates of  $0.42 \text{ kg NO}_2^- \text{-N m}^{-3} \text{ d}^{-1}$  were easily achieved with  $\text{NO}_2^- \text{-N/TAN}$  ratios around unity. Moreover, nitrate production was as low as  $0.005 \text{ kg NO}_3^- \text{-N m}^{-3} \text{ d}^{-1}$  and the effluent was biomass-free, making the MBR a suitable reactor system for preceding an anaerobic ammonium oxidation reactor within an integrated autotrophic nitrogen removal process. Application of microfiltration guarantees a strongly decreased solids wash-in into the anaerobic ammonium oxidation stage, thereby decreasing solids accumulation and reducing the risk of biomass dilution and reactor failure due to the slow growth of the anoxic consortium. In addition, high concentrations of suspended biomass were maintained in the partial nitrification MBR by complete sludge retention. With this reactor configuration, the maximum volumetric loading rate is not limited by the maximum growth rate of the ammonium oxidizers, as is the case in chemostat systems (e.g., SHARON process). By uncoupling HRT and SRT, biomass washout at high dilution rates is circumvented. Higher production rates for nitrite are likely to be achieved by further decreasing the HRT, therefore requiring more membrane surface per reactor volume to increase the MBR effluent flux.

### $K_{L,a}$ Determination and Model Calibration Via Batch Experiments

Within WEST, applied aeration profiles with varying values for the gas–liquid oxygen transfer coefficient ( $K_{L,a}$ ) are introduced via the input file. The  $K_{L,a}$  was influenced by operating temperature, stirring rate, and airflow rate. Reactor temperature ( $30.0^\circ\text{C}$ ) and stirring rate (200 rpm) were maintained constant during all experiments. Figure 3 shows the calibration curve for the  $K_{L,a}$  under different airflow rates. The relationship between oxygen transfer coefficient ( $K_{L,a}$ ,  $\text{d}^{-1}$ ) and airflow rate ( $Q_A$ ,  $\text{L m}^{-3} \text{ min}^{-1}$ ) was found to be  $K_{L,a} = 0.55 Q_A + 102$ . Higher  $K_{L,a}$  values were found when the empty MBR was filled with tap water. Solids and dissolved salts tended to lower the gas–liquid oxygen transfer when aerating the MBR biomass feeding on the reject water. This is expressed within the  $\alpha$ -value, which is defined as the ratio of the oxygen transfer coefficient for the MBR ( $K_{L,a}$ ) to the oxygen transfer coefficient for tap water ( $K_{L,a}^*$ ). An  $\alpha$ -value of  $0.52 \pm 0.04$  was found for airflow rates between  $47\text{--}520 \text{ L m}^{-3} \text{ min}^{-1}$  at a solids concentration of  $10.3 \text{ g MLSS L}^{-1}$ . A comparable  $\alpha$ -value of 0.6 was determined for full-scale municipal MBRs with solids concentrations of  $12 \text{ g MLSS L}^{-1}$  (Cornel et al., 2003). Higher solids concentrations resulted in lower  $\alpha$ -values. Similarly, at very high biomass concen-

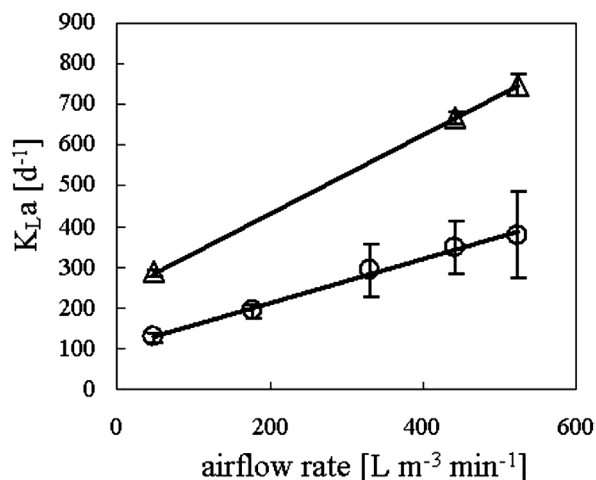


**Figure 3.** Relationship between airflow rate and  $K_{L,a}$  determined for MBR medium ( $\circ$ ) and clean tap water ( $\Delta$ ), with reactor conditions controlled at  $T = 30^\circ\text{C}$ , stirring rate = 200 rpm, at  $V = 1.5 \text{ L}$  and  $\text{MLSS} = 10.3 \text{ g L}^{-1}$ .

trations in a biofilm airlift suspension reactor exceeding  $17 \text{ g VSS L}^{-1}$ , Garrido et al. (1997) showed that the  $K_{L,a}$  was negatively influenced by an ever-increasing biomass concentration due to a decreased oxygen hold-up.

Airflow rates were continuously monitored with rotameters allowing the calculation of the  $K_{L,a}$  at any point during the reactor run. To compensate for the lower solids concentration at the beginning of the run, the  $\alpha$ -value was corrected with a factor 1.1–1.3 according to the observations of Cornel et al. (2003).

The kinetic conversion model was specifically calibrated for the oxygen-limited partial nitrification process in the MBR. Operational characteristics of this process are rather different from those encountered in most nitrification systems. It is expected that these differences are reflected in the composition of the nitrifying community, including some of their kinetic and stoichiometric parameters. For example, the low DO concentration puts a selective pressure upon the system for organisms coping well with limited oxygen availability, while high sludge ages allow the propagation of slow-growing organisms. A two-step nitrification model in WEST accurately described the batch oxidation profiles of the respirometry experiments. Resulting parameter estimations ( $T = 30.0^\circ\text{C}$ ;  $\text{pH} = 7.90$ ) determined experimentally for the ammonium oxidizing biomass were  $\mu^{\text{max}} = 2.02 \text{ d}^{-1}$ ,  $K_O = 0.24 \text{ mg DO L}^{-1}$ ,  $K_{\text{NH}_3} = 0.85 \text{ mg NH}_3 \text{ L}^{-1}$ . Compared to general literature data for the oxygen affinity constant ( $K_O = 0.6 \text{ mg DO L}^{-1}$  at  $30^\circ\text{C}$ ; Wiesmann, 1994) a somewhat lower value was measured, which could be explained by the fact that the MBR (low DO, high SRT) selects for ammonium oxidizers having a higher oxygen affinity. The affinity constant for ammonia substrate is very high compared to literature values ( $K_{\text{NH}_3} = 0.034 \text{ mg NH}_3 \text{ L}^{-1}$  at  $30^\circ\text{C}$ , Wiesmann, 1994), most likely due to the fact that the organisms were exposed to high ammonium concentrations and as such not

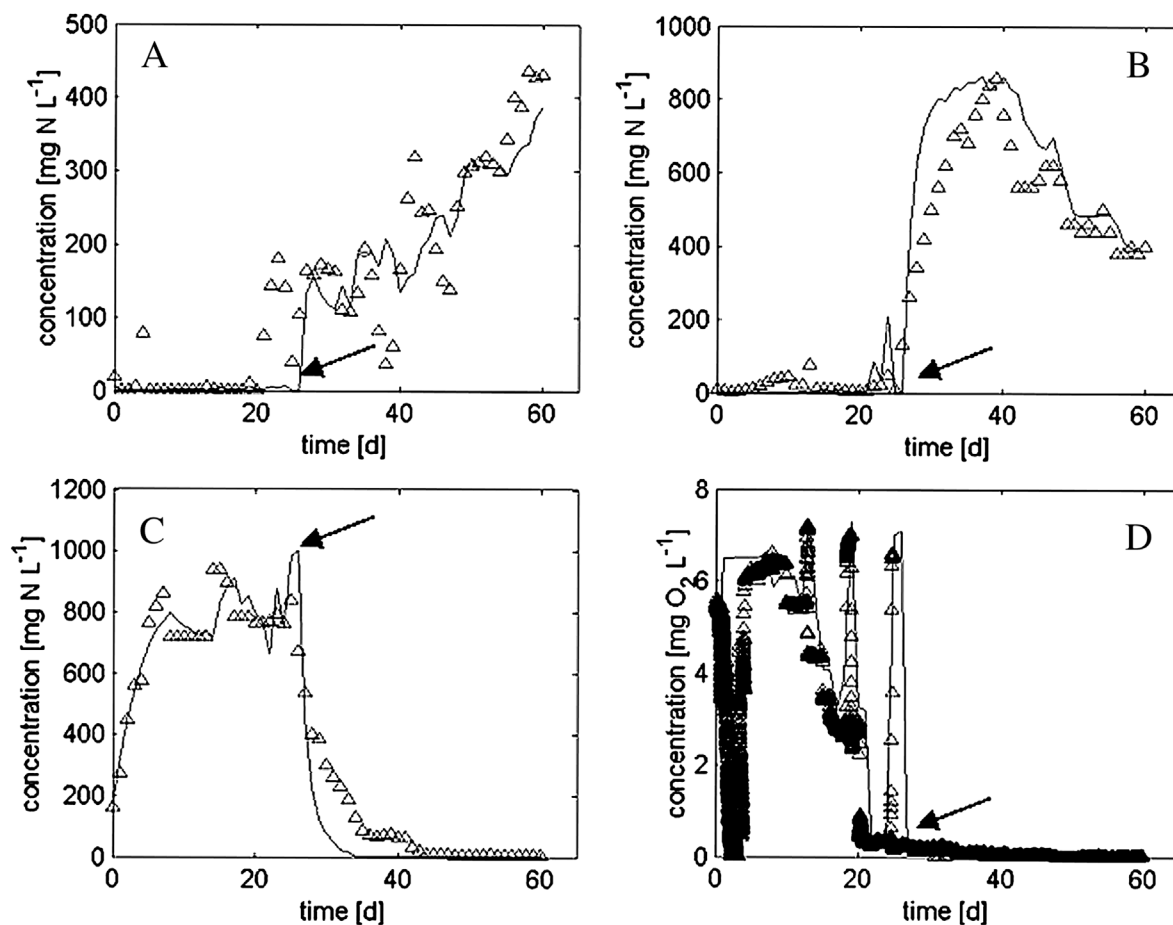
selected for their substrate affinity. With respect to this, a similar high affinity constant ( $K_{\text{NH}_3} = 0.65 \text{ mg NH}_3 \text{ L}^{-1}$  at  $30^\circ\text{C}$  and  $\text{pH } 8$ ) was found for ammonium oxidizer growth under SHARON conditions (Hellinga et al., 1999). Parameter estimation for nitrite oxidation was, however, difficult because of too low oxygen uptake rates when dosing  $\text{KNO}_2$ . At steady-state operation of the process, the amount of nitrite oxidizers was simply too low, which can be explained by the fact that by maintaining low DO their growth rate was severely suppressed. This will also be illustrated by the simulation results in the following model validation section. Therefore, standard literature values were chosen for nitrite oxidizer kinetics (Wiesmann, 1994). Since nitrite oxidizers are also exposed to high substrate concentrations, a high substrate affinity constant for nitrous acid was assumed. Stoichiometric and kinetic parameters are summarized in the Appendix (Tables A.III and A.IV).

### Model Validation: Modeling the Start-Up of the Partial Nitritation Process

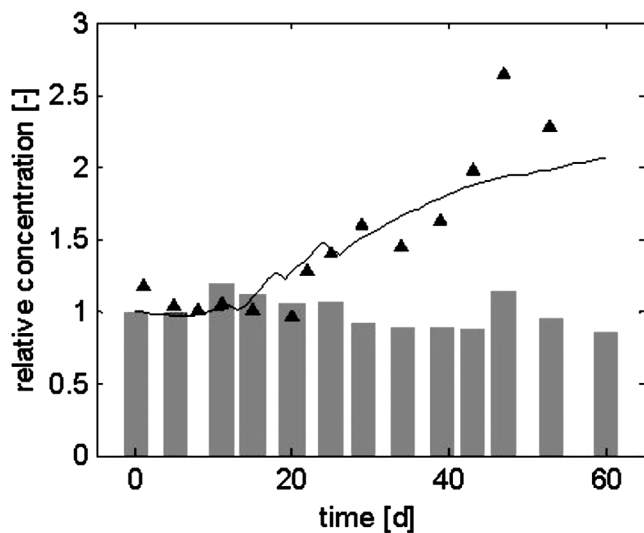
A comparison between modeled and measured data for the TAN,  $\text{NO}_2^-$ -N,  $\text{NO}_3^-$ -N and DO concentrations is given in

Figure 4. Reactor loading rates and airflow rates were changed as pointed out above (Fig. 2a). The modeled concentrations agree well with the measured concentrations. Low DO concentrations were measured during the first 4 days of the start-up, because the membrane of the oxygen sensor was fouled with biomass. The loading rate was set to zero (no addition of sludge reject water) on days 12, 19, and 25 resulting in lower oxygen uptake rates and a temporary high bulk DO, which can be seen both from the experimental and modeled data. On day 25 the effect of no wastewater addition is also reflected in a decreased concentration of ammonium and nitrite, and an increased nitrate concentration.

The modeled concentration of particulate COD (particulate COD = inert particulate COD + biomass particulate COD) also agrees well with the measured values, although the measurement frequency was lower compared to the nitrogen compounds (Fig. 5). As expected, operating the MBR without sludge waste (infinite SRT) resulted in the accumulation of inert particulate COD ( $X_I$ ), which can be seen from the start-up simulation data in Figure 6. It was assumed that 15% of biomass decay products was inert particulate matter (Henze et al., 2000). However, no signi-



**Figure 4.** Measured ( $\Delta$ ) and modeled (—) MBR effluent concentrations of TAN (A),  $\text{NO}_2^-$ -N (B),  $\text{NO}_3^-$ -N (C) and DO (D) after decreasing HRT and  $K_{L,a}$  as outlined in Figure 2a. The effect of a zero loading rate on the concentrations (day 25) is indicated by arrows.



**Figure 5.** Measured ( $\blacktriangle$ ) and modeled (—) accumulation of particulate COD and evolution of VSS (gray bars). Concentrations of COD and VSS are shown relative to their initial concentration at the time of inoculation.

ficant accumulation of biomass VSS was measured (Fig. 5) which also becomes obvious from the simulation data for concentrations of the ammonium oxidizers, nitrite oxidizers, and heterotrophs (Fig. 6). The total biomass concentration was rather constant through the start-up period with moderate fluctuations due to substrate availability. The amount of ammonium oxidizing biomass ( $X_{NH}$ ) was negatively affected by the events of a zero loading rate on days 19 and 25. The concentration of nitrite oxidizers ( $X_{NO}$ ) was steadily decreasing after reducing the airflow rate and thereby limiting the oxygen supply. Estimated model based calculations of the biomass concentration after 200 days of stable operation at constant reactor conditions ( $T = 30^\circ\text{C}$ ;  $\text{pH} = 7.9$ ;  $\text{TAN}_{\text{influent}} = 870 \text{ mg N L}^{-1}$ ;  $\text{HRT} = 1 \text{ d}$ ;  $K_L a = 150 \text{ d}^{-1}$ ) revealed that  $X_{NH}$  was  $0.41 \text{ g COD L}^{-1}$  while  $X_{NO}$  was nearly zero. Nitrite oxidizers were completely out-competed at low DO concentrations (which resulted from a combination of high loading rate and a low airflow rate), but from a physiological point of view the additional effect of inhibiting high concentrations FA could not be discriminated from the low DO effect. However, introduction of a FA inhibition term in the kinetics of the ammonium and nitrite oxidizers had no influence on the model output of nitrogen compounds or biomass concentration. Therefore, the simplified model was used with Monod terms for microbial growth. As such, oxygen limitation and low DO were suggested as the main factors for maintaining nitrite accumulation. Heterotrophic bacteria were able to persist under the indicated reactor conditions and were only a fraction (15%) of the estimated active biomass concentration.

Based on the agreement of experimental and modeled data it was concluded that the conversion model was properly validated, allowing further predictions with model simulations.

### Simulation of the Effect of Temperature, $K_L a$ and HRT on Ammonium and Nitrite Conversion

Simulations with the validated kinetic model were performed to demonstrate the possibility of obtaining stable effluent concentrations, which are suited for subsequent autotrophic nitrogen removal via anaerobic ammonium oxidation. In a first series of simulations, the effect of operating reactor temperature on ammonium and nitrite conversion was investigated. Simulations were carried out at 15, 20, 25, 30, and  $35^\circ\text{C}$  over a 200 days period with all other parameters kept constant ( $\text{pH} = 7.9$ ;  $\text{TAN}_{\text{influent}} = 870 \text{ mg N L}^{-1}$ ;  $\text{HRT} = 1 \text{ d}$ ). The airflow rate was also constant resulting in constant  $K_L a$  values (123, 150, 182, 222, and  $270 \text{ d}^{-1}$  for the five different temperatures, respectively). After 200 days of simulated operation, the effluent nitrogen concentrations and reactor biomass concentrations were in steady state. The absence of nitrite oxidizing activity under oxygen limitation was reflected in both the simulated nitrate concentrations and the simulated nitrite oxidizing biomass concentration, independent of reactor temperature (Fig. 7). Nitrate concentrations and nitrite oxidizer biomass concentrations were always below  $0.005 \text{ mg N L}^{-1}$  and  $0.002 \text{ g COD L}^{-1}$ , respectively. As such, high temperatures are not a prerequisite for stable process operation in terms of preventing nitrate production. The formation of nitrate during partial nitrification is disadvantageous since nitrate is not further removed in the anaerobic ammonium oxidation reactor. In chemostat systems without sludge retention such as the SHARON process, nitrate production is circumvented by washing out the nitrite oxidizers, which have a lower growth rate than ammonium oxidizers at high temperatures between  $30\text{--}40^\circ\text{C}$  (Hellinga et al., 1998). In practice, a temperature of  $35^\circ\text{C}$  is needed to operate the SHARON process at its maximum rate, which often requires reactor

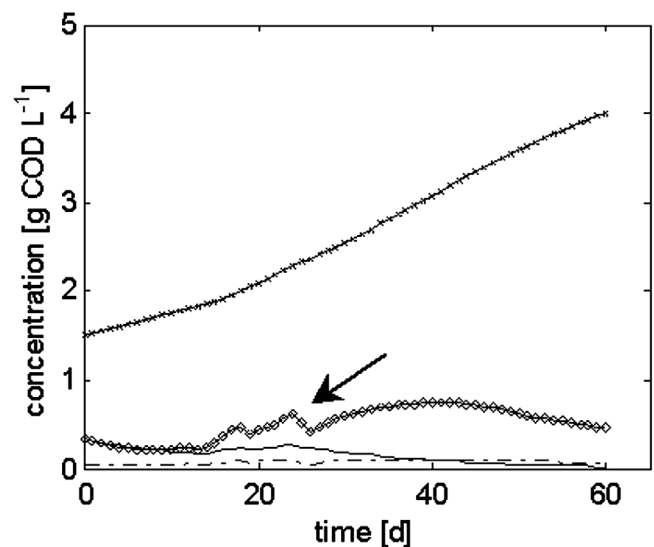


**Figure 6.** Simulation of inert particulate COD ( $\times$ ) accumulation and growth of heterotrophic (— — —), ammonium oxidizing ( $\diamond$ ) and nitrite oxidizing (—) biomass. The effect of a zero loading rate on the concentration of ammonium oxidizing biomass (day 25) is indicated by an arrow.

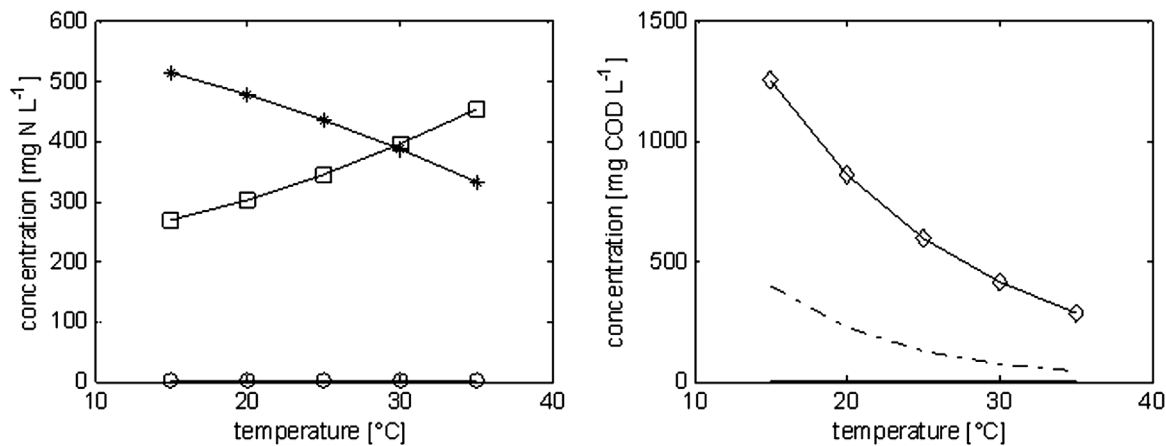


**Figure 7.** Simulated effect of an operating reactor temperature between 15 and 35°C on the steady state concentrations of TAN (\*), NO<sub>2</sub>-N (□) and NO<sub>3</sub>-N (○) (left) and ammonium oxidizing (◇), nitrite oxidizing (—) and heterotrophic biomass (---) (right) at  $K_{L,a} = 150 \text{ d}^{-1}$ .

insulation or an external heating system (van Kempen et al., 2001). In the chemostat approach stable nitrite accumulation is achieved when the reactor temperature is at least 30°C (van Dongen et al., 2001). At lower temperatures, nitrite oxidizer activity is likely to reappear and ammonium conversion rates are significantly decreased (Fux et al., 2002). Using the MBR for oxygen-limited partial nitrification, operating at a lower temperature is possible (no reactor heating and insulation required) while still maintaining a low HRT. More specifically, flexibility towards reactor temperature is desirable in these cases where the warm sludge reject water can't be treated directly from the digester drain point and is cooled down to ambient temperatures, which can be critical in colder climates.

Biomass decay rates were found to be much higher at elevated temperature (see the Appendix), resulting in lower concentrations of active biomass (Fig. 7). In the simulations at 30°C, the total amount of autotrophic and heterotrophic biomass was only 45% of its value at 20°C.

Reactor temperature had a considerable influence on ammonium conversion, while nitrite conversion to nitrate

remained unaffected (Fig. 7). At a temperature below 30°C, for example at 20°C, ammonium conversion to nitrite is only  $0.3 \text{ kg N m}^{-3} \text{ d}^{-1}$  resulting in a sub-optimal NO<sub>2</sub>-N/TAN effluent ratio of 0.63. By simulating an increased HRT of 1.45 d, or an increased  $K_{L,a}$  of  $195 \text{ d}^{-1}$  at this temperature of 20°C, the NO<sub>2</sub>-N/TAN ratio in the effluent can be restored again to an optimal value of 1. Thus, working under continuous oxygen limitation and constant reactor pH, the rate of ammonium conversion at a given loading rate is only determined by temperature and  $K_{L,a}$ . This was also demonstrated in a series of process simulations at different values for  $K_{L,a}$  (obtained by varying the airflow rate) shown in Figure 8 for two different temperatures. The ammonium conversion rate and nitrite concentration increased with increasing  $K_{L,a}$ -values up to about  $325 \text{ d}^{-1}$  and  $400 \text{ d}^{-1}$  at 20°C and 30°C, respectively. At higher  $K_{L,a}$ -values ammonium was limiting and oxygen became increasingly available for the nitrite oxidizing biomass resulting in the production of nitrate. Nitrite conversion was complete at  $K_{L,a}$ -values above  $500 \text{ d}^{-1}$  and  $590 \text{ d}^{-1}$  at 20°C and 30°C, respectively. The oxygen availability for the nitrite oxidizers

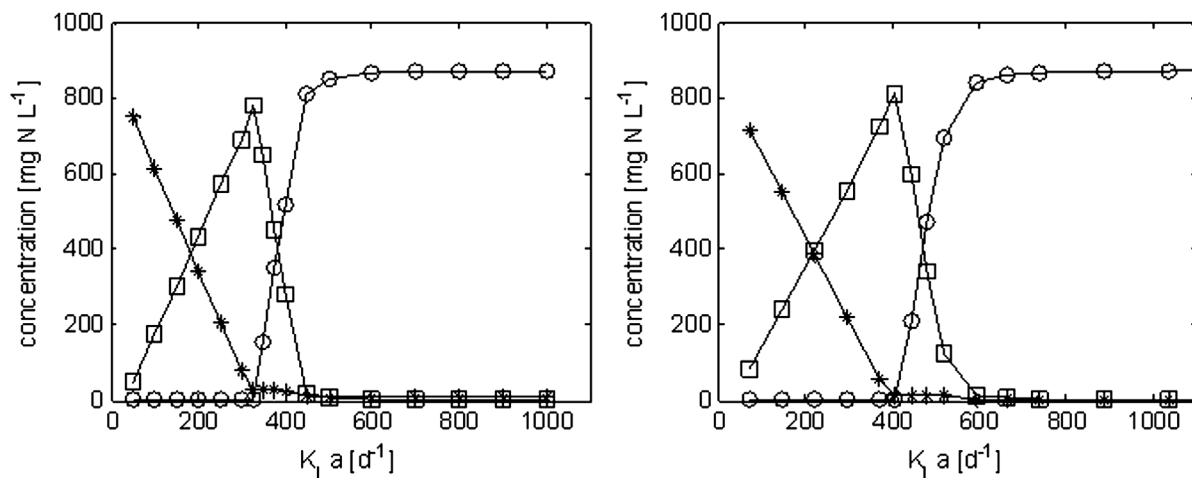


**Figure 8.** Simulated effect of an oxygen transfer coefficient between 40 and  $1000 \text{ d}^{-1}$  on the steady-state concentrations of TAN (\*), NO<sub>2</sub>-N (□) and NO<sub>3</sub>-N (○) at  $T = 20^\circ\text{C}$  (left) and  $30^\circ\text{C}$  (right).

can be reduced again by increasing the loading rate and thus the oxygen uptake by the ammonium oxidizers.

In a second series of simulations, the dimensions of the partial nitrification process were designed by a combination of HRT and  $K_L a$ . The required reactor volume and aeration capacity are determined by HRT and  $K_L a$ , respectively. The key features of the process are: reactor operation under oxygen limitation, preventing nitrite oxidation and limiting ammonium conversion that results in the generation of effluents with a  $\text{NO}_2^- \text{-N/TAN}$  ratio of 1, making them ideally suited for subsequent treatment via anaerobic ammonium oxidation. Shorter HRTs require higher  $K_L a$ -values to obtain ideal effluent ratios (Fig. 9). The effect of reactor temperature on the necessary  $K_L a$  is more pronounced at HRTs below 1 day. From these simulations it was noted that a partial nitrification process with a HRT as short as 0.25 days should be possible, thereby achieving optimal ammonium conversion. Further shortening of the HRTs would require an unrealistic high aeration capacity. A short HRT or high volumetric loading rate means more costs for additional membrane surface since a higher effluent flux needs to be generated. However, these costs should be weighed against a strongly decreased reactor volume. With respect to nitrification processes in chemostat systems (e.g., SHARON process with  $\text{HRT} = \text{SRT}$ ) the required reactor volume for generating an Anammox suited effluent can be largely decreased.

### Simulation of the Effect of SRT on the Accumulation of Particulate Matter

In a third and final series of simulations the influence of SRT on the accumulation of particulate matter was investigated. So far, the SRT was always set infinite (complete sludge retention and no sludge waste) in both the experimental runs and in the simulations. An infinite SRT and subsequent

increasing inert particulate COD concentration (Fig. 5) is, however, not beneficial for the gas-liquid oxygen transfer, requiring more aeration energy to obtain the same oxygen input (or reach the same  $K_L a$ -value). Also an ever-increasing solids concentration could have a detrimental effect on the membrane filtration performance. Steady-state simulations were performed at SRT of 10, 25, 50, 75, and 100 days and constant reactor operating conditions ( $T = 30^\circ\text{C}$ ;  $\text{pH} = 7.9$ ;  $\text{TAN}_{\text{influent}} = 870 \text{ mg N L}^{-1}$ ;  $\text{HRT} = 1 \text{ d}$ ;  $K_L a = 222 \text{ d}^{-1}$ ). The resulting total particulate COD, inert particulate COD and concentration of ammonium oxidizing biomass in the MBR as a function of the SRT is shown in Figure 10. As expected, the total and inert particulate COD concentration increased with increasing SRT. The concentration of ammonium oxidizing biomass was nearly unaffected by the SRT since growth of the ammonium oxidizers was largely determined by the availability of substrate (in casu oxygen) and by the operating temperature. Lower SRTs showed only a small diluting effect on the nitrifying biomass. In addition, the effluent ratio  $\text{NO}_2^- \text{-N/TAN}$  was not affected by increasing the sludge age, indicating the possibility of the MBR to be operated at different SRTs. In practice, operating the MBR at a SRT somewhere between 50 and 75 days should be appropriate in terms of minimized sludge waste production with still sufficient oxygen transfer.

### CONCLUSIONS

A nitrifying membrane-assisted bioreactor (MBR) treating sludge reject water was operated under low DO with the purpose of generating a stable partial nitrification process. Decreasing the HRT and the airflow rate during start-up limited the oxygen transfer and resulted in oxygen limitation. Nitrite oxidizer activity consequently decreased and ammonium conversion was adjusted to 53% of the incoming

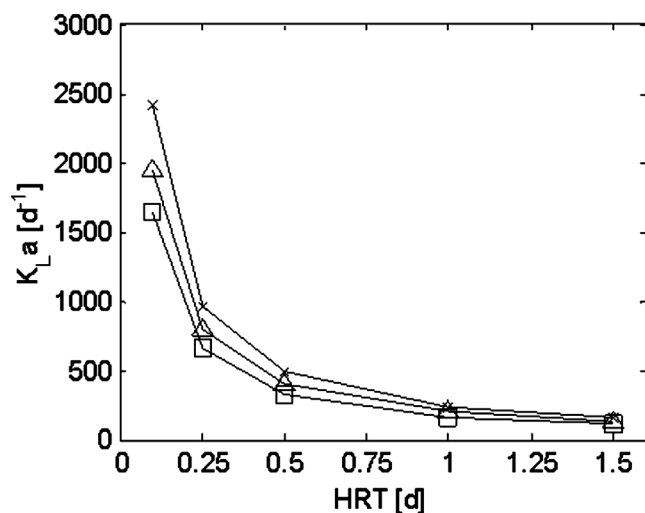


**Figure 9.** Simulated effect of the hydraulic residence time (HRT) on the volumetric oxygen transfer coefficient ( $K_L a$ ) needed to produce a reactor effluent suitable for further anaerobic ammonium oxidation, at 15 (□), 25 (△), 35 (×) °C.

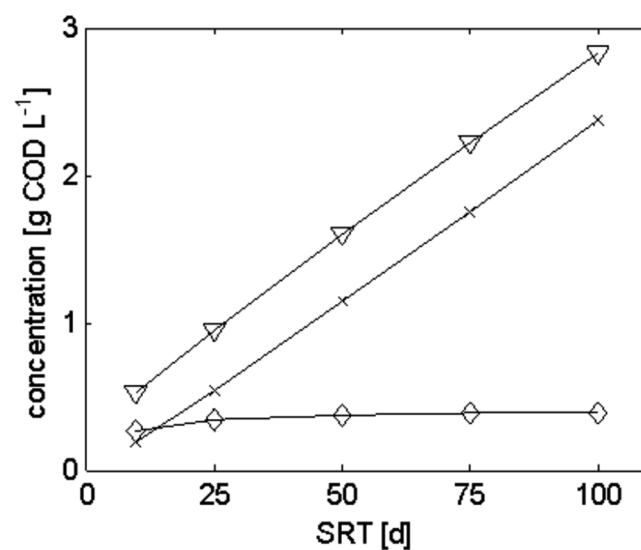


**Figure 10.** Total particulate COD (▽), inert particulate COD (×) and concentration of ammonium oxidizing biomass (◇) as function of the SRT.

loading rate. These start-up phenomena were accurately described using a newly developed two-step nitrification model within WEST, which was calibrated with in situ measurements of kinetic parameters for ammonium oxidizer growth. The model was properly validated and was used for simulation under different operational conditions. This allows further optimization of the oxygen-limited partial nitrification process and could provide an excellent tool for scenario analysis when upscaling is considered. Based on these results, the MBR for oxygen-limited partial nitrification is proposed as a suitable configuration to precede reactor systems for anaerobic ammonium oxidation. The process features a biomass free effluent, a high loading rate, and flexibility towards operating reactor temperature. It should be possible to operate the process for side-stream treatment of sludge reject water at ambient temperatures of 20°C and with a HRT down to 0.25 days, corresponding with a volumetric loading rate of 3.7 kg N m<sup>-3</sup> d<sup>-1</sup>.

## APPENDIX

In this Appendix the complete stoichiometric matrix, together with the kinetic expressions and the values for

the different parameters are given. For description of the Peterson matrix format, the reader is referred to Henze et al. (2000). The kinetic expressions are shown in Table A.II. The complete stoichiometric matrix is given in Tables A.I(a) and A.I(b). The values for the different parameters are given in Table A.III and A.IV.

### Calculation of Actual Substrates for Ammonium and Nitrite Oxidizer Growth

The concentrations of ammonia (S<sub>NH3</sub>) and nitrous acid (S<sub>HNO2</sub>) are calculated from the concentrations of TAN (S<sub>NH</sub>) and NO<sub>2</sub><sup>-</sup>-N (S<sub>NO2</sub>) as follows:

$$S_{NH3} = \frac{S_{NH}}{1 + \frac{10^{-pH}}{K_e^{NH}}} \quad (1)$$

$$S_{HNO2} = \frac{S_{NO2}}{1 + \frac{K_e^{NO}}{10^{-pH}}} \quad (2)$$

where pH is the reactor pH, K<sub>e</sub><sup>NH</sup> (= e<sup>-6344/(273 + T)</sup>) is the acidity constant of the ammonium/ammonia equilibrium

**Table A.I(a).** Stoichiometric matrix of soluble components.

Component No.	1	2	3	4	5	6
Name	Oxygen	Substrate	Ammonium	Nitrite	Nitrate	Nitrogen gas
Symbol	S <sub>O</sub>	S <sub>S</sub>	S <sub>NH</sub>	S <sub>NO2</sub>	S <sub>NO3</sub>	S <sub>N2</sub>
Unit	mg O <sub>2</sub> L <sup>-1</sup>	mg COD L <sup>-1</sup>	mg N L <sup>-1</sup>	mg N L <sup>-1</sup>	mg N L <sup>-1</sup>	mg N L <sup>-1</sup>
1 Hydrolysis of entrapped organics		1				
2 Growth of X <sub>H</sub>	-(1-Y <sub>H</sub> )/Y <sub>H</sub>	-1/Y <sub>H</sub>	-i <sub>nbm</sub>			
3 Decay of X <sub>H</sub>			i <sub>nbm</sub> -f <sub>p</sub> i <sub>nxi</sub>			
4 Growth of X <sub>H</sub> on NO <sub>3</sub> <sup>-</sup>		-1/Y <sub>H,NO3</sub>	-i <sub>nbm</sub>	(1-Y <sub>H,NO3</sub> ) / (1.14 Y <sub>H,NO3</sub> )	-(1-Y <sub>H,NO3</sub> ) / (1.14 Y <sub>H,NO3</sub> )	
5 Growth of X <sub>H</sub> on NO <sub>2</sub> <sup>-</sup>		-1/Y <sub>H,NO2</sub>	-i <sub>nbm</sub>	-(1-Y <sub>H,NO2</sub> ) / (1.71 Y <sub>H,NO2</sub> )		(1-Y <sub>H,NO2</sub> ) / (1.71 Y <sub>H,NO2</sub> )
6 Growth of X <sub>NH</sub>	-(3.43-Y <sub>NH</sub> )/Y <sub>NH</sub>		-1/Y <sub>NH</sub> -i <sub>nbm</sub>	1/Y <sub>NH</sub>		
7 Decay of X <sub>NH</sub>			i <sub>nbm</sub> -f <sub>p</sub> i <sub>nxi</sub>			
8 Growth of X <sub>NO</sub>	-(1.14-Y <sub>NH</sub> )/Y <sub>NH</sub>		-i <sub>nbm</sub>	-1/Y <sub>NO</sub>	1/Y <sub>NO</sub>	
9 Decay of X <sub>NO</sub>			i <sub>nbm</sub> -f <sub>p</sub> i <sub>nxi</sub>			

**Table A.I(b).** Stoichiometric matrix of particulate components.

Component No.	7	8	9	11	12
Name	Heterotrophs	Ammonium oxidizers	Nitrite oxidizers	Slowly degradable substrate	Inert particulates
Symbol	X <sub>H</sub>	X <sub>NH</sub>	X <sub>NO</sub>	X <sub>S</sub>	X <sub>i</sub>
Unit	mg COD L <sup>-1</sup>	mg COD L <sup>-1</sup>			
1 Hydrolysis of entrapped organics				-1	
2 Growth of X <sub>H</sub> on O <sub>2</sub>	1				
3 Decay of X <sub>H</sub>	-1			(1-f <sub>i</sub> )	f <sub>i</sub>
4 Growth of X <sub>H</sub> on NO <sub>3</sub> <sup>-</sup>	1				
5 Growth of X <sub>H</sub> on NO <sub>2</sub> <sup>-</sup>	1				
6 Growth of X <sub>NH</sub>		1			
7 Decay of X <sub>NH</sub>		-1		(1-f <sub>i</sub> )	f <sub>i</sub>
8 Growth of X <sub>NO</sub>			1		
9 Decay of X <sub>NO</sub>			-1	(1-f <sub>i</sub> )	f <sub>i</sub>

**Table A.II.** Kinetic equations.

Process	Process rate equation
1. Hydrolysis of entrapped organics	$k_H \frac{X_S/X_H}{K_X+X_S/X_H} X_H$
2. Growth of $X_H$	$\mu_H^{\max} e^{(T-T_r)} \frac{S_o}{K_{O,H} + S_o} \frac{S_S}{K_{S,H} + S_S} X_H$
3. Decay of $X_H$	$b_H e^{(T-T_r)} X_H$
4. Growth of $X_H$ on $\text{NO}_3^-$	$\mu_H^{\max} e^{(T-T_r)} \eta_{\text{NO}_3} \frac{K_{O,H}}{K_{O,H} + S_o} \frac{S_{\text{NO}_3}}{K_{\text{NO}_3,H} + S_{\text{NO}_3}} \frac{S_S}{K_{S,H} + S_S} X_H$
5. Growth of $X_H$ on $\text{NO}_2^-$	$\mu_{\text{NH}}^{\max} e^{(T-T_r)} \eta_{\text{NO}_2} \frac{K_{O,H}}{K_{O,H} + S_o} \frac{S_{\text{NO}_2}}{K_{\text{NO}_2,H} + S_{\text{NO}_2}} \frac{S_S}{K_{S,H} + S_S} X_H$
6. Growth of $X_{\text{NH}}$	$\mu_{\text{NH}}^{\max} e^{(T-T_r)} \frac{S_o}{K_{O,\text{NH}} + S_o} \frac{S_{\text{NH}_3}}{K_{\text{NH}_3,\text{NH}} + S_{\text{NH}_3}} \cdot X_{\text{NH}}$
7. Decay of $X_{\text{NH}}$	$b_{\text{NH}} e^{(T-T_r)} X_{\text{NH}}$
8. Growth of $X_{\text{NO}}$	$\mu_{\text{NO}}^{\max} e^{(T-T_r)} \frac{S_o}{K_{O,\text{NO}} + S_o} \frac{S_{\text{HNO}_2}}{K_{\text{HNO}_2,\text{NO}} + S_{\text{HNO}_2}} \cdot X_{\text{NO}}$
9. Decay of $X_{\text{NO}}$	$b_{\text{NO}} e^{(T-T_r)} X_{\text{NO}}$

$(\text{NH}_4^+ \leftrightarrow \text{NH}_3 + \text{H}^+)$  and  $K_c^{\text{NO}} (= e^{-2300/(273 + T)})$  is the acidity constant of the nitrite/nitrous acid equilibrium ( $\text{HNO}_2 \leftrightarrow \text{NO}_2^- + \text{H}^+$ ). For both equilibrium constants a temperature dependency as proposed by Anthonisen et al. (1976) was used.

(Henze et al., 2000). This allows the investigation of the performance of the reactor at different temperatures:

$$k(T) = k(T_r) e^{\theta(T-T_r)} \quad (3)$$

### Temperature Dependency of Kinetic Parameters

For the kinetic parameters a temperature dependency was incorporated according to an Arrhenius type equation

where  $k(T)$  is the kinetic parameter (maximum specific growth rate  $\mu^{\max}$  or decay coefficient  $b$ ) at the actual temperature  $T$ ,  $T_r$  is the reference temperature (20°C) and  $\theta$  is the Arrhenius constant. The Arrhenius constant for

**Table A.III.** Stoichiometric parameters.

Symbol	Definition	Value	Unit	Reference
$Y_{\text{H}_2\text{O}}$	Heterotrophic yield on oxygen	0.52	$\text{g COD g}^{-1} \text{COD}$	Henze et al. (2000)
$Y_{\text{H},\text{NO}_3}$	Heterotrophic yield on $\text{NO}_3$	0.44	$\text{g COD g}^{-1} \text{COD}$	Henze et al. (2000)
$Y_{\text{H},\text{NO}_2}$	Heterotrophic yield on $\text{NO}_2$	0.44	$\text{g COD g}^{-1} \text{COD}$	Henze et al. (2000)
$Y_{\text{NH},\text{O}}$	Autotrophic yield of $X_{\text{NH}}$	0.15	$\text{g COD g}^{-1} \text{N}$	Wiesmann (1994)
$Y_{\text{NO},\text{O}}$	Autotrophic yield of $X_{\text{NO}}$	0.041	$\text{g COD g}^{-1} \text{N}$	Wiesmann (1994)
$f_i$	Production of $X_i$ from decay	0.15	$\text{g COD g}^{-1} \text{COD}$	Henze et al. (2000)
$i_{\text{Nxi}}$	N content of $X_i$	0.02	$\text{g N g}^{-1} \text{COD}$	Henze et al. (2000)
$I_{\text{nbm}}$	N content of biomass	0.0583	$\text{g N g}^{-1} \text{COD}$	Henze et al. (2000)

**Table A.IV.** Kinetic parameters.

Symbol	Definition	Value (at 30°C and pH 7.9)	Unit	Reference
$k_h$	Maximum specific hydrolysis rate	3	$\text{g COD g}^{-1} \text{COD d}^{-1}$	Henze et al. (2000)
$K_X$	Saturation constant for slowly biodegradable substrate	0.03	$\text{g COD g}^{-1} \text{COD}$	Henze et al. (2000)
$\mu_H^{\max}$	Maximum growth rate of $X_H$	8.72	$\text{d}^{-1}$	Henze et al. (2000)
$K_{O,H}$	Saturation constant for $S_o$ of $X_H$	0.2	$\text{g O}_2 \text{ m}^{-3}$	Henze et al. (2000)
$K_{S,H}$	Saturation constant for $S_S$ of $X_H$	50	$\text{g COD m}^{-3}$	Adapted from Henze et al. (2000)
$b_H$	Decay rate of $X_H$	2.32	$\text{d}^{-1}$	Adapted from Henze et al. (2000)
$\eta_{\text{NO}_3}$	Anoxic reduction factor	0.6	—	Adapted from Henze et al. (2000)
$\eta_{\text{NO}_2}$	Anoxic reduction factor	0.6	—	Adapted from Henze et al. (2000)
$K_{\text{NO}_3,H}$	Saturation constant for $S_{\text{NO}_3}$ of $X_H$	1	$\text{g N m}^{-3}$	Adapted from Henze et al. (2000)
$K_{\text{NO}_2,H}$	Saturation constant for $S_{\text{NO}_2}$ of $X_H$	1	$\text{g N m}^{-3}$	Adapted from Henze et al. (2000)
$\mu_{\text{NH}}^{\max}$	Maximum growth rate of $X_{\text{NH}}$	2.02	$\text{d}^{-1}$	This study
$K_{O,\text{NH}}$	Saturation constant for $S_o$ of $X_{\text{NH}}$	0.235	$\text{g O}_2 \text{ m}^{-3}$	This study
$K_{\text{NH}_3,\text{NH}}$	Saturation constant for $S_{\text{NH}_3}$ of $X_{\text{NH}}$	0.85	$\text{g NH}_3 \text{ m}^{-3}$	This study
$b_{\text{NH}}$	Decay rate of $X_{\text{NH}}$	0.19	$\text{d}^{-1}$	Adapted from Wiesmann (1994)
$\mu_{\text{NO}}^{\max}$	Maximum growth rate of $X_{\text{NO}}$	1.36	$\text{d}^{-1}$	Wiesmann (1994)
$K_{O,\text{NO}}$	Saturation constant for $S_o$ of $X_{\text{NO}}$	1.5	$\text{g O}_2 \text{ m}^{-3}$	Wiesmann (1994)
$K_{\text{HNO}_2,\text{NO}}$	Saturation constant for $S_{\text{HNO}_2}$ of $X_{\text{NO}}$	$8.723 \cdot 10^{-4}$	$\text{g HNO}_2 \text{ m}^{-3}$	Wiesmann (1994)
$b_{\text{NO}}$	Decay rate of $X_{\text{NO}}$	0.092	$\text{d}^{-1}$	Adapted from Wiesmann (1994)

autotrophs can be calculated with the activation energy ( $E_{act}$ ) of the autotrophic biomass (Hao et al., 2002):

$$\theta = E_{act}/(R 293 (T + 273)) \quad (4)$$

where  $R$  is the universal gas constant ( $8.31 \text{ J mol}^{-1} \text{ K}^{-1}$ ). Since the activation energies of aerobic ammonium and nitrite oxidation according to literature are 68 and 44  $\text{kJ mol}^{-1}$ , respectively (Jetten et al., 1999) the  $\theta$  values were calculated to be 0.094 and 0.061, respectively. For heterotrophs the  $\theta$  values for maximum specific growth rate  $\mu_{H}^{\max}$  and decay coefficient  $b_H$  were assumed to be 0.069 and 0.11, respectively as proposed by Henze et al. (2000).

Also the oxygen transfer coefficient ( $K_L a$ ) and the oxygen saturation concentration ( $C_S$ ) were temperature dependent (ASCE, 1996):

$$K_L a(T) = K_L a(T_r) \phi^{(T_r - T)} \quad (5)$$

$$C_S(T) = 14.65 - 0.41 T + 7.99 \cdot 10^{-3} T^2 - 7.78 \cdot 10^{-5} T^3 \quad (6)$$

where  $\phi$  is the temperature correction factor (1.04).

Gurkan Sin is gratefully acknowledged for helping with the model construction within WEST.

## References

- American Public Health Association, Inc. (APHA). 1992. Standard methods for the examination of water and wastewater, 18th ed. New York: American Public Health Association, Inc.
- American Society of Civil Engineers (ASCE). 1996. Standard guidelines for in-process oxygen transfer testing. New York: American Society of Civil Engineers.
- Abeling U, Seyfried CF. 1992. Anaerobic-aerobic treatment of high-strength ammonium wastewater - nitrogen removal via nitrite. *Water Sci Technol* 26(5-6):1007-1015.
- Anthonisen AC, Loehr RC, Prakasam TBS, Srinath EG. 1976. Inhibition of nitrification by ammonia and nitrous acid. *J Water Poll Control* 48(5): 835-852.
- Bernet N, Dangcong P, Delgènes J-P, Moletta R. 2001. Nitrification at low oxygen concentration in biofilm reactor. *J Environ Eng-ASCE* 127(3): 266-271.
- Cornel P, Wagner M, Krause S. 2003. Investigation of oxygen transfer rates in full scale membrane bioreactors. *Water Sci Technol* 47(1):313-319.
- Fux C, Boehler M, Huber F, Brunner I, Siegrist H. 2002. Biological treatment of ammonium-rich wastewater by partial nitrification and subsequent anaerobic ammonium oxidation (anammox) in a pilot plant. *J Biotechnol* 99(3):295-306.
- Garrido JM, van Benthum WAJ, van Loosdrecht MCM, Heijnen JJ. 1997. Influence of dissolved oxygen concentration on nitrite accumulation in abiofilm airlift suspension reactor. *Biotechnol Bioeng* 53(2):168-178.
- Han D-W, Yun H-J, Kim D-J. 2001. Autotrophic nitrification and denitrification characteristics of an upflow biological aerated filter. *J Chem Technol Biot* 76(11):1112-1116.
- Hao X, Heijnen JJ, van Loosdrecht MCM. 2002. Sensitivity analysis of a biofilm model describing a one-stage completely autotrophic nitrogen removal (CANON) process. *Biotechnol Bioeng* 77(3):266-277.
- Hellinga C, Schellen AAJC, Mulder JW, van Loosdrecht MCM, Heijnen JJ. 1998. The Sharon process: An innovative method for nitrogen removal from ammonium-rich waste water. *Water Sci Technol* 37(9): 135-142.
- Hellinga C, van Loosdrecht MCM, Heijnen JJ. 1999. Model based design of a novel process for nitrogen removal from concentrated flows. *Math Comput Model* 5(4):351-371.
- Henze M, Gujer W, Matsuo T, van Loosdrecht M. 2000. Activated sludge models ASM1, ASM2, ASM2d and ASM3, scientific and technical reports. London: IWA Publishing.
- Jetten MSM, Strous M, van de Pas-Schoonen K, Schalk J, van Dongen UGJM, van de Graaf AA, Logemann S, Muyzer G, van Loosdrecht MCM, Kuenen JG. 1999. The anaerobic oxidation of ammonium. *FEMS Microbiol Rev* 22(5):421-437.
- Jetten MSM, Schmid M, Schmidt I, Wubben M, van Dongen U, Abma W, Slijkers O, Revsbech NP, Beaumont HJE, Ottosen L et al. 2002. Improved nitrogen removal by application of new nitrogen-cycle bacteria. *Re/Views Environ Sci Bio/Technol* 1(1):51-63.
- Liebig T, Wagner M, Bjerrum L, Denecke M. 2001. Nitrification performance and nitrifier community composition of a chemostat and a membrane-assisted bioreactor for the nitrification of sludge reject water. *Bioproc Biosyst Eng* 24(4):203-210.
- Mulder A, van de Graaf AA, Robertson LA, Kuenen JG. 1995. Anaerobic ammonium oxidation discovered in a denitrifying fluidized bed reactor. *FEMS Microbiol Ecol* 16(3):177-184.
- Mulder JW, van Loosdrecht MCM, Hellinga C, van Kempen R. 2001. Full-scale application of the Sharon process for the treatment of rejection water of digested sludge dewatering. *Water Sci Technol* 43(11):127-134.
- Pollice A, Tandoi V, Lestingi C. 2002. Influence of aeration and sludge retention time on ammonium oxidation to nitrite and nitrate. *Water Res* 36(10):2541-2546.
- Ruiz G, Jeison D, Chamy R. 2003. Nitrification with high nitrite accumulation for the treatment of wastewater with high ammonia concentration. *Water Res* 37(6):1371-1377.
- Siegrist H. 1996. Nitrogen removal from digester supernatant—Comparison of chemical and biological methods. *Water Sci Technol* 34(1-2):399-406.
- Turk O, Mavinic DS. 1989. Maintaining nitrite buildup in a system acclimated to free ammonia. *Water Res* 23(1):1383-1388.
- van de Graaf AA, de Bruijn P, Robertson LA, Jetten MSM, Kuenen JG. 1997. Metabolic pathway of anaerobic ammonium oxidation on basis of  $^{15}\text{N}$ -studies in a fluidized bed reactor. *Microbiol* 143(Part 7): 2415-2421.
- van Dongen U, Jetten MSM, van Loosdrecht MCM. 2001. The Sharon-Anammox process for treatment of ammonium rich wastewater. *Water Sci Technol* 44(1):153-160.
- van Kempen R, Mulder JW, Uijterlinde CA, van Loosdrecht MCM. 2001. Overview: Full scale experience of the SHARON process for treatment of rejection water of digested sludge dewatering. *Water Sci Technol* 44(1):145-152.
- Vanhooren H, Meirlaen J, Amerlinck Y, Claeys F, Vangheluwe H, Vanrolleghem PA. 2003. WEST: Modeling biological wastewater treatment. *J Hydroinform* 5(1):27-50.
- Verstraete W, Phillips S. 1998. Nitrification-denitrification processes and technologies in new contexts. *Environ Poll* 102(Suppl. 1):717-726.
- Voets JP, Vanstaen H, Verstraete W. 1975. Removal of nitrogen from highly loaded nitrogenous wastewater. *J Water Poll Control* 47(2): 394-398.
- Wiesmann U. 1994. Biological nitrogen removal from wastewater. In: Fiechter A, editor. *Advances in Biochemical Engineering / Biotechnology*, vol. 51. Berlin: Springer-Verlag. p 113-154.
- Wyffels S, Boeckx P, Pynaert K, Verstraete W, Van Cleemput O. 2003. Sustained nitrite accumulation in a membrane-assisted bioreactor (MBR) for the treatment of ammonium rich wastewater. *J Chem Technol Biot* 78(4):412-419.
- Yang L, Alleman JE. 1992. Investigation of batchwise nitrite build-up by an enriched nitrification culture. *Water Sci Technol* 26(5-6): 997-1005.